

Symmetry of the spin Hamiltonian for herbertsmithite: a spin- $\frac{1}{2}$ kagomé lattice

Oren Ofer and Amit Keren

Physics Department, Technion, Israel Institute of Technology, Haifa 32000, Israel

We present magnetization measurements on oriented powder of $\text{ZnCu}_3(\text{OH})_6\text{Cl}_2$ along and perpendicular to the orienting field. We find a dramatic difference in the magnetization between the two directions. It is biggest at low measurement fields H or high temperatures. We show that the difference at high temperatures must emerge from Ising-like exchange anisotropy. This allows us to explain muon spin rotation data at $T \rightarrow 0$ in terms of an exotic ferromagnetic ground state.

PACS numbers: 75.50.Lk, 75.10.Nr

The synthesis of the herbertsmithite [$\text{ZnCu}_3(\text{OH})_6\text{Cl}_2$] [1] has led to a renewed interest in the frustrated spin- $\frac{1}{2}$ Heisenberg model on the kagomé lattice. This system has a highly degenerate ground state [2] and any small perturbation to the Hamiltonian can severely affect the ground state manifold. The perturbations can be: exchange anisotropy [3], bond anisotropy [4, 5], transverse field [6, 7], Dzyaloshinsky-Moriya Interaction (DMI) [8, 9, 10], or longer range interactions [11]. Therefore, numerous theoretical directions have been taken to predict the low-temperature behavior of the kagomé system, and some of them were particularly applied to magnetization and other measurements of the herbertsmithite [10][12].

This mithite is exciting since Cu ions create a spin- $\frac{1}{2}$ magnetic kagomé layer separated by non magnetic Zn atoms from the adjacent layers. The compound was found to be a quantum spin liquid with no broken continuous symmetry but gapless excitations [13, 14, 15, 16, 17]. At high temperatures the inverse susceptibility obeys a Curie-Weiss (CW) law, $\chi = C/(T + \theta)$, where C is the Curie constant and the CW temperature $\theta = 314$ K. Below ~ 75 K a sharp increase in the susceptibility occurs, deviating from the ideal kagomé Heisenberg model [18]. This upturn was accounted for by DMI

[10, 19] or anisotropy in the bonds [4, 7]. It was also suggested that impurities from a Zn/Cu substitution play a significant role in the low-temperature susceptibility [17][20, 21]. However, free impurities, or interacting impurities that generate an additional ferromagnetic Curie-Weiss law [10][12], have been shown not to describe this upturn completely. In fact, Rietveld refinement of our sample showed no Zn/Cu substitution within the experimental resolution [22]. The sample is made by the same procedure and group as the samples in Refs. [15] and [23]. Finally, different local probes such as muon [14], O, [17] Cu, and Cl [23] nuclear magnetic resonance, and electron spin resonance [19] suggest different behavior of the susceptibility below ~ 50 K. Thus, there is still no agreement on the interactions that control the magnetic properties of herbertsmithite.

In fact, since it is only available as a powder, the symmetries of its spin Hamiltonian are not known. To clarify these symmetries we present magnetization measurements on oriented powder of $\text{ZnCu}_3(\text{OH})_6\text{Cl}_2$ along (\hat{z}) and perpendicular (\perp) the orienting field. The symmetry of the interactions are probed at high temperatures where impurities are not expected to contribute to the susceptibility even if they do exist, and all probes roughly agree.

The orientation was done by curing $\text{ZnCu}_3(\text{OH})_6\text{Cl}_2$ powder overnight with Stycast in a field of 8 T at room temperature. The samples were cured in a Teflon form producing a ball 6 mm in diameter. During the first 40 minutes of the orientation, a shaking mechanism was applied to the sample form. A particularly small amount of powder was used to avoid saturating the Stycast and eliminating powder residues at the bottom of the ball. We prepared a second “test” sample in the same manner, but this time without orientation. We refer to the second ball as the powder sample. The mass of $\text{ZnCu}_3(\text{OH})_6\text{Cl}_2$ in the ball is known only roughly and the absolute value of the molar magnetization is not accurate. We also prepared a ball made of Stycast only. All samples were measured in a gelatin capsule.

In Fig. 1 we plot the x-ray diffraction from the powder and oriented samples. For these measurements a separate surface perpendicular to the orienting field was prepared and used. The Bragg peak intensities are shown in the figure. In the oriented case the (002) and (006) peaks

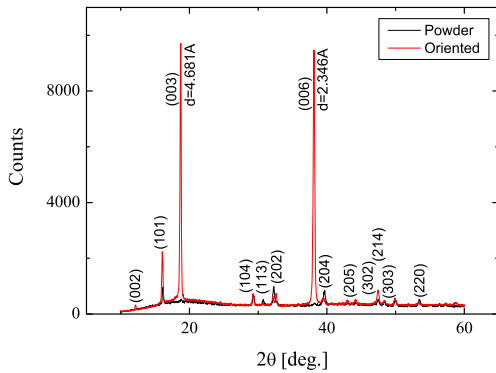


FIG. 1: (Color online) X-ray diffraction of powder (black) and oriented powder (gray) from a surface perpendicular to the orienting field.

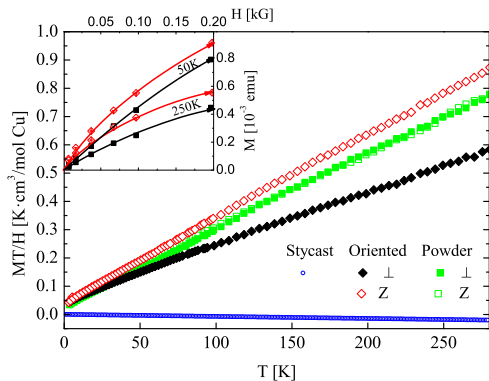


FIG. 2: (Color online) Normalized magnetization $M/H \equiv \chi$ times the temperature versus temperature at external field of 400 G for oriented sample (diamonds) in two directions, powder sample (squares) in two directions as if it was oriented, and stycast sample (open circles). The inset shows the magnetization as a function of applied field for two different temperatures and directions for low fields.

increased dramatically, while many of the other peaks did not. This x-ray picture shows a high degree of orientation such that the c direction is parallel to the field. The level of orientation will be discussed further below.

DC magnetization measurements, M , were performed using a Cryogenic SQUID magnetometer in two configurations. One configuration ‘ z ’ is when the orienting and the applied (SQUID) fields coincide, ($H \parallel c$). The other configuration ‘ \perp ’ is when the ball is rotated by 90° and thus the applied field is in the kagomé plane, ($H \perp c$). In Fig. 2 we present MT/H of the two samples, powder and oriented balls. In the rest of this paper we use χ to indicate the normalized magnetization M/H (and not $\partial M/\partial H$). These measurements were taken at $H = 400$ G. The measurements are conducted as follows: we first measured the powder sample and then the oriented sample in both configurations. Finally, we repeated the powder measurements for a second time, but rotated the powder ball as if it was oriented. All powder measurements collapse into a single curve, as expected, demonstrating the reproducibility of the measurement. The Stycast sample showed a very small diamagnetic signal which is also depicted in Fig. 2. The core diamagnetic susceptibility of $\text{ZnCu}_3(\text{OH})_6\text{Cl}_2$ is $-16.7 \times 10^{-5} \text{ cm}^3/\text{mole}$ [24]. The Van-Vleck contribution is expected to be of the same order of magnitude, but with a positive sign [25]. Both are much smaller than the measured χ at room temperature of $1 \times 10^{-3} \text{ cm}^3/\text{mole}$.

In Fig. 2 no special energy scale is found in either one of the measurements. The only indication of an interaction between spins is the fact that χT for both directions and the powder decreases with decreasing T . χT of the powder is smaller than $\chi_z T$ and larger than $\chi_\perp T$ of the oriented sample. However, a comparison of the absolute value of χ of the powder and the oriented sample is not accurate. We did try to have an equal amount of sample

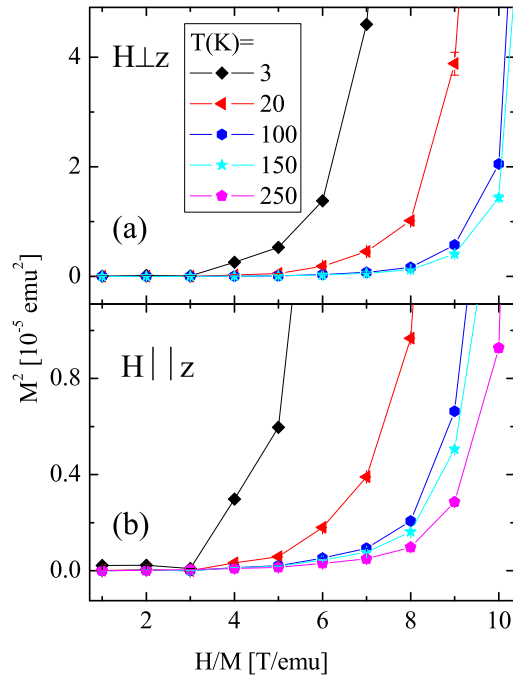


FIG. 3: (Color online) An Arrott plot showing M^2 versus H/M at various temperatures in the perpendicular direction (a) and parallel direction (b).

in both balls but there is no telling how successful we were. A more relevant comparison is between χ in the different directions of the oriented sample; $\chi_z T$ increases faster than $\chi_\perp T$, and at room temperature $\chi_z = 1.6\chi_\perp$. Thus the ratio between the z and \perp directions increases as the temperature increases.

In the inset of Fig. 2 we show the magnetization as a function of H for two different temperatures and directions. The magnetization is beginning to show signs of saturation, suggesting contribution from ferromagnetic impurities. To check this possibility we present in Fig. 3 an Arrott plot [26]. This plot takes advantage of the high field data. At a ferromagnetic transition, $M^2(T_c)$ is expected to be a linear function of H/M . We found no evidence for such linear behavior. In fact, $M^2(T)$ is independent of H/M near the origin as expected when the ferromagnetic critical temperature is lower than the available temperature. This indicates the lack of ferromagnetic impurities in our measurements.

In Fig. 4 we plot χ^{-1} versus temperature for two fields, 2000 and 100 G and for the two orientations. In the inset of Fig. 4(b) we plot the χ^{-1} at low temperatures ($T < 50$ K); clearly, χ_z linearizes at $T \sim 30$ K whereas χ_\perp linearizes at a much higher temperature ($T \sim 100$ K). θ , and C in arbitrary units are extracted from a linear fit of the high-temperature ($150 < T < 280$ K) data to

$\chi_{\perp,z}^{-1} = (T + \theta_{\perp,z})/C_{\perp,z}$. The fits are shown by the solid line.

In Fig. 5 we plot $\theta_{\perp,z}$, and $\sqrt{C_{\perp,z}}$ which is proportional to the $g_{\perp,z}$ factor (if the sample was fully oriented) versus the applied field. θ_{\perp} increases slowly with decreasing applied field and saturates below 400 G. On the other hand, θ_z increases rapidly below 2 kG. The Curie constant has a similar behavior. The powder average of $\theta_{\perp,z}$ at low fields does not reconcile with $\theta \sim 300$ K measured in a powder and there must be some extrinsic contribution to the normalized magnetization in the partially aligned samples at low fields. However, we have no evidence that this contribution is due to impurities.

In contrast, at high fields, $H > 2$ kG, θ of the two directions is hardly distinguishable and on the order of the powder value. In addition, useful information can be extracted from the CW temperature only if it is obtained by measurements at $T \gtrsim \theta$. Therefore, we concentrate on the results obtained by $H \geq 2$ kG, as shown in the inset of Fig. 5. At 2 kG the ratio of $\sqrt{C_z/C_{\perp}} = 1.179(6)$ and $\theta_z/\theta_{\perp} = 1.23(1)$.

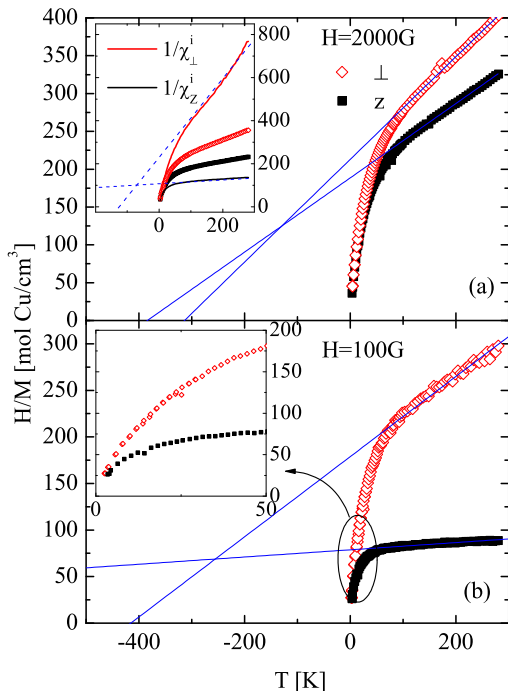


FIG. 4: (Color online) Inverse normalized magnetization $H/M \equiv \chi^{-1}$ versus temperature at $H = 2$ kG (a) and at $H = 100$ G (b). The solid lines are linear fits to the high temperature (> 150 K) data. (a) inset displays the inverse of the normalized magnetizations $1/\chi_z$ (black squares) and $1/\chi_{\perp}$ (gray diamonds), and the inverse intrinsic normalized magnetization $1/\chi_z^i$ (black line) and $1/\chi_{\perp}^i$ (gray line) obtained from Eq. 1. The dashed lines demonstrate that $\theta_z < \theta_z^i$ and $\theta_{\perp} > \theta_{\perp}^i$. In the inset of (b) we plot the low-temperature behavior of χ^{-1} at 100 G.

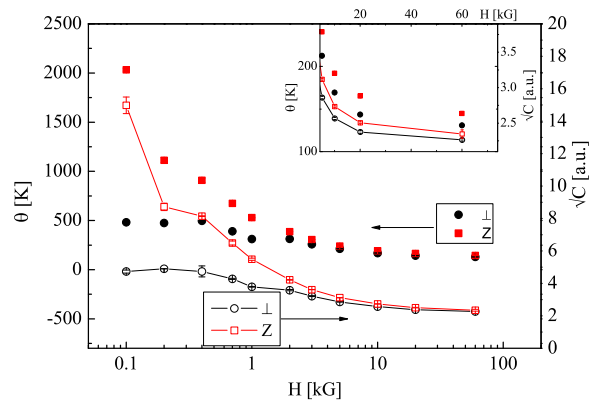


FIG. 5: (Color online) The Curie-Wiess temperatures (filled symbols) and square root of the Curie constant (open symbols) of the oriented sample perpendicular to (black) and in the kagomé plane (gray). The inset show a zoom on the high field data.

In order to convert the measured χ presented above to the intrinsic normalized magnetization χ^i in different directions, it is important to estimate the level of orientation. This can be done using the x-ray data. The ratio of the x-ray intensity (I) from the powder $R = I(00h)/I(kk0)$ represents the signal intensity ratio between the two kinds of plane. Let's assume that there are N grains composed of two sets, αN that can orient perfectly with the field, and $(1 - \alpha)N$ that are not effected by the field at all since they are made of a few crystalline, for example. We further define β as the probability that a particular plane will contribute to the scattering intensity in a powder. After orientation the x-ray intensity ratio between the same planes would be $R' = [\alpha R + \beta(1 - \alpha)R]/\beta(1 - \alpha)$. We can estimate β from the width of the peaks which is 0.2° out of 180 , thus $\beta \sim 0.001$. Using R and R' of the (006) and (220) we find $\alpha = 0.25$. This level of orientation is in agreement with Imai *et al.*[23].

In an oriented sample we expect

$$\chi_{z,\perp} = (1 - \alpha) \left(\frac{1}{3}\chi_z^i + \frac{2}{3}\chi_{\perp}^i \right) + \alpha\chi_{z,\perp}^i. \quad (1)$$

This relation could be inverted to produce $\chi_{z,\perp}^i$. In the inset of Fig. 4(a) we present both $1/\chi_{z,\perp}$ and $1/\chi_{z,\perp}^i$ for the normalized magnetization data taken at $H = 2$ kG. New intrinsic CW temperatures $\theta_{z,\perp}^i$ could be obtained from $1/\chi_{z,\perp}^i$ as demonstrated by the dashed lines. $\theta_{z,\perp}^i$ represent the CW temperature as if the sample was fully oriented. Although α is just an estimate of the level of orientation, the important point is that $\theta_z^i > \theta_z$ and $\theta_{\perp}^i < \theta_{\perp}$.

We now turn to discuss the possible origin of the χ anisotropy in terms of superexchange anisotropy and

DMI. The DMI Hamiltonian is given by,

$$\mathcal{H} = \sum_{\langle i,j \rangle} JS_i \cdot S_j + \mathbf{D}_{ij} \cdot (\mathbf{S}_i \times \mathbf{S}_j) \quad (2)$$

where \mathbf{D}_{ij} is a vector assigned to each bond. In the mean field approximation ($\mathbf{S}_j \rightarrow \mathbf{M}/g\mu_B$) this Hamiltonian is written as

$$\mathcal{H} = g\mu_B \sum_i \mathbf{S}_i \cdot \mathbf{H}^{eff}$$

where

$$\mathbf{H}^{eff} = \frac{Z}{(g\mu_B)^2} (J\mathbf{M} + \mathbf{D} \times \mathbf{M}) + \mathbf{H} \quad (3)$$

$\mathbf{D} = (1/Z) \sum_j \mathbf{D}_{ij}$, and Z is the number of neighbors. Special attention must be taken for the convention of the ij bond direction since it sets the direction of \mathbf{D}_{ij} [10]. The magnetization satisfy the equation

$$\mathbf{M} = \frac{C}{T} \left(\frac{Z}{(g\mu_B)^2} (J\mathbf{M} + \mathbf{D} \times \mathbf{M}) + \mathbf{H} \right) \quad (4)$$

where $C = (g\mu_B)^2 S(S+1)/(3k_B)$ is the Curie constant. Up to first order in \mathbf{D}

$$\mathbf{M} = \frac{C}{(T - \theta_{cw})} \left(\mathbf{I} + \frac{1}{T - \theta_{cw}} \mathbf{A} \right) \mathbf{H}. \quad (5)$$

where $\theta_{cw} = CZJ/(g\mu_B)^2$ and

$$\mathbf{A} = \frac{CZ}{(g\mu_B)^2} \begin{pmatrix} 0 & -D_z & D_y \\ D_z & 0 & -D_x \\ -D_y & D_x & 0 \end{pmatrix}. \quad (6)$$

In particular

$$M_{z,\perp} = \frac{C}{(T - \theta_{cw})} H_{z,\perp} \quad (7)$$

Therefore, \mathbf{D}_{ij} does not contribute to the CW law.

In contrast, the superexchange anisotropy Hamiltonian is given by

$$\mathcal{H} = \sum_{\langle i,j \rangle} J_z S_i^z \cdot S_j^z + J_\perp \mathbf{S}_i^\perp \cdot \mathbf{S}_j^\perp. \quad (8)$$

In this case, if the sample was perfectly oriented, we would have $\theta_{z,\perp} = J_{z,\perp}/k_B$. Since our sample is not perfectly oriented, our high-temperature high field linear fits of $\chi_{\perp,z}^{-1}$ measures a lower bound on J_z and an upper bound on J_\perp .

The lower bound on J_z is larger than the upper bound on J_\perp . Despite the fact that measurements of χ_z and χ_\perp are contaminated with χ_\perp^i and χ_z^i respectively, as indicated by Eq. 1, the conclusion $J_z > J_\perp$ is unavoidable. It is robust even against possible core and Van-Vleck corrections. Thus herbertsmithite has an Ising-like exchange anisotropy. This, however, is not the end of the story. If

$J_z > J_\perp$, we would expect $\chi_z < \chi_\perp$, in contrast to observation. Therefore, to explain the high χ in the z direction we must invoke an anisotropic g factor as well.

In the classical ground state of antiferromagnets on the kagomé lattice with exchange anisotropy, the spins are coplanar and two angles between spins φ on each triangle obey $\cos \varphi = -J_z/(J_z + J_\perp)$. The third angle completes the circle. This condition maintains the ground state macroscopic degeneracy. Nevertheless, unlike in the Heisenberg case, there is a critical temperature T_c below which an exotic ferromagnetic order exists with finite total magnetization, but no sublattice long-range order [27]. Upon cooling through T_c the magnetization increases abruptly and continuously down to $T \rightarrow 0$ where it saturates [28]. In zero field, domains can be formed, but a small applied magnetic field will stabilize the moment. The powder average of the moment projection on the field direction is given by the value

$$\langle \mathbf{M} \cdot \hat{\mathbf{H}} \rangle = \frac{\mu_B}{6} (1 + 2 \cos \varphi) \quad (9)$$

per spin.

We believe that this ferromagnetic order contributes to the observed χ at $T \rightarrow 0$ by transverse field (TF) muon spin rotation (μ SR) experiment [14]. In μ SR, impurities, if they exist, are expected to contribute to the muon line width while most of the sample contributes to the line shift. In what follows we examine what part of the μ SR shift can be explained by exchange anisotropy only. A complete understanding will of course require taking DMI interaction into account as well.

The μ SR measurements were done at a field of $H = 2$ kG and the shift K in the muon rotation frequency as a function of temperature was measured. This shift is a consequence of the sample magnetization; therefore, K is expected to be proportional to normalized magnetization. The high temperature data are used to calibrate the proportionality constant between K and χ [14]. The data are reproduced in Fig. 6. χ increases sharply with decreasing temperatures between ~ 10 K and ~ 1 K and saturates below $T \sim 200$ mK at a value of $\chi = 15.7(5) \times 10^{-3} \text{ cm}^3/\text{mol Cu}$. This χ mounts to an average moment of $0.006\mu_B$ per Cu, in the direction of the applied 2 kG field. Solving Eq. 9 for the anisotropies gives $J_z/J_\perp = 1.06$. In Fig. 6 we present simulations described in Ref. [27], for $J_z/J_\perp = 1.04$ and $J_z/J_\perp = 1.08$ showing similar behaviour as the experiment. For this type of exchange anisotropy the expected $T_c/J_\perp = 0.03$ as shown in the inset of Fig. 6 also taken from Ref. [27]. For $J_\perp \simeq 200$ K we expect $T_c = 6$ K. This temperature is at the center of the sharp rise of χ . Thus we see that both the saturation and the increase of χ detected by μ SR could be qualitatively explained by exchange anisotropy.

To summarize, our measurements in $\text{ZnCu}_3(\text{OH})_6\text{Cl}_2$ reveal an anisotropic intrinsic spin magnetization with $\chi_z^i > \chi_\perp^i$ possibly due to anisotropic g factor. At fields above 2 kG a CW temperature can be consistently de-

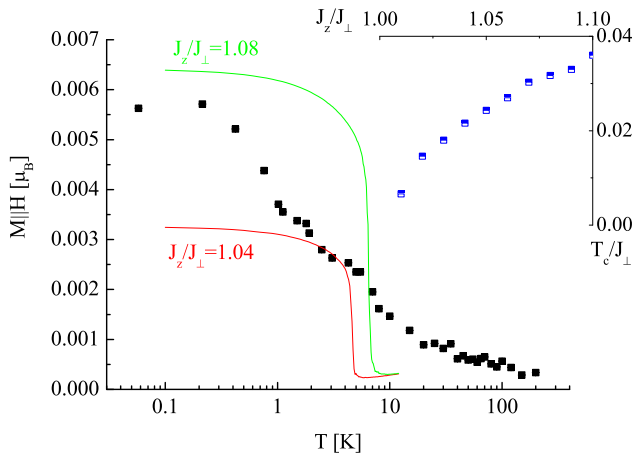


FIG. 6: (Color online) A plot of the magnetization detected by muon spin rotation versus temperature (black squares), and simulation data for antiferromagnetic kagomé lattice with Ising-like exchange anisotropy as in Ref. [28] (gray lines). In the inset the normalized critical temperature versus the exchange anisotropy is shown.

terminated in two different directions. By mean-field approximations we were able to show that this phenomenon can be explained only by anisotropic super-exchange constants where $J_z > J_\perp$. This anisotropy can explain the main features of the susceptibility determined by μ SR.

We are grateful to E. A. Nytko and D. G. Nocera for providing us with the sample, and to S. Tanaka, S. Miyashita, and N. Kawashima for providing us with the simulation results shown in Fig. 6. We acknowledge helpful discussions with Young S. Lee, Rajiv Singh, Marcos Rigol, and John Chalker. We also would like to thank the Israel - U. S. Binational Science Foundation for supporting this research.

-
- [1] Matthew P. Shores, Emily A. Nytko, Bart M. Bartlett and Daniel G. Nocera, *J. Am. Chem. Soc.*, **127**, 13462 (2005).
- [2] A.P. Ramirez, *Annu. Rev. Mater. Sci.* **24**, 453 (1994).
- [3] Oleg A. Starykh and Leon Balents, *Phys. Rev. Lett.* **93** 127202 (2004).
- [4] Philippe Sindzingre, cond-mat/0707.4264
- [5] T. Yavors’kii, W. Apel, H.-U. Everts, *Phys. Rev. B* **76**, 064430 (2007)
- [6] R. Moessner, S.L. Sondhi and P. Chandra, *Phys. Rev. Lett.* **84**, 4457 (2000).
- [7] Chyh-Hong Chern, Mitsuaki Tsukamoto, *Phys. Rev. B* **77**, 172404 (2008).
- [8] M. Elhajal, B. Canals and C. Lacroix, *Phys. Rev. B* **66**, 014422 (2002).
- [9] Daniel Grohol, Kittiwit Matan, Jin-Hyung Cho, Seung-Hun Lee, Jeffrey W. Lynn, Daniel G. Nocera and Young S. Lee, *Nature Materials* **4**, 323 (2005).
- [10] Marcos Rigol and Rajiv R.P. Singh, *Phys. Rev. B* **76**, 184403 (2007).
- [11] M.D. Núñez-Regueiro, C. Lacroix and B. Canals, *Phys. Rev. B* **54** R736 (1996).
- [12] Grégoire Misguich and Philippe Sindzingre, *Eur. Phys. J. B* **59** 305, (2007).
- [13] S.-H.Lee, H. Kikuchi, Y. Qiu, B. Lake, Q. Huang, K. Habicht and K. Kiefer, *Nature Materials* **6**, 853 (2007).
- [14] Oren Ofer, Amit Keren, Emily A. Nytko, Matthew P. Shores, Bart M. Bartlett, Daniel G. Nocera, Chris Baines, Alex Amato, cond-mat/0610540.
- [15] J.S. Helton, K. Matan, M. P. Shores, E. A. Nytko, B. M. Bartlett, Y. Yoshida, Y. Takano, A. Suslov, Y. Qiu, J.-H. Chung, D. G. Nocera, and Y. S. Lee, *Phys. Rev. Lett.* **98** 107204 (2007).
- [16] P. Mendels, F. Bert, M. A. de Vries, A. Olariu, A. Harrison, F. Duc, J. C. Trombe, J. S. Lord, A. Amato and C. Baines, *Phys. Rev. Lett.* **98**, 077204 (2007).
- [17] A. Olariu, P. Mendels, F. Bert, F. Duc, J. C. Trombe, M. A. de Vries, and A. Harrison, *Phys. Rev. Lett.* **100** 087202 (2008).
- [18] T. Nakamura and S. Miyashita, *Phys. Rev. B* **52**, 9174 (1995).
- [19] A. Zorko, S. Nellutla, J. van Tol, L. C. Brunel, F. Bert, F. Duc, J. C. Trombe, M. A. de Vries, A. Harrison and P. Mendels, *Phys. Rev. Lett.* **101** 026405 (2008).
- [20] F. Bert, S. Nakamae, F. Ladieu, D. L’Hote, P. Bonville, F. Duc, J.-C. Trombe, P. Mendels, *Phys. Rev. B* **76** 132411 (2007).
- [21] M.A.de Vries, K.V.Kamenev, W.A.Kockelmann, J.Sanchez-Benitez, A.Harrison, *Phys. Rev. Lett.* **100**, 157205 (2008).
- [22] Emily A. Nytko, Ph. D. thesis, Massachusetts Institute of Technology, 2008.
- [23] T. Imai, E. A. Nytko, B. M. Bartlett, M. P. Shores and D. G. Nocera, *Phys. Rev. Lett.* **100** 077203, (2008).
- [24] P. W. Selwood, *Magnetochemistry*, 2nd ed. (Interscience, New York, 1956), p. 78.
- [25] D. C. Johnston and J. H. Cho, *Phys. Rev. B* **42**, 8710 (1990).
- [26] A. Arrott, *Phys. Rev.* **108**, 1394 (1957).
- [27] A. Kuroda and S. Miyashita, *J. Phys. Soc. Japan* **64**, 4509 (1995).
- [28] Shu Tanaka and Seiji Miyashita, *J. Phys.: Condens. Matter* **19**, 145256 (2007).